

# A Compact 16-Port Fractal Shaped Slot Antenna Array for 5G Smart Phone Communications

Nayab Khan<sup>1</sup>, Muhammad Bilal<sup>2</sup>, Raza Ali<sup>2</sup>, Akbar Khan<sup>2</sup>

<sup>1</sup> Chief Minister Delivery Unit, CM Secretariat, Quetta, 87300 Pak

<sup>2</sup>Department of Electrical Engineering, Baluchistan University of Information Technology and Management Sciences, Quetta, Pakistan

Corresponding author: Nayab Khan (e-mail: [nayabkhattak93@gmail.com](mailto:nayabkhattak93@gmail.com))

**ABSTRACT** - In this manuscript, a 16-port compact multi-antenna array for fifth generation communications is presented. The proposed antenna system is designed to facilitate high data rate communication through the implementation of MIMO (multiple-input-multiple-output) wireless technology. Efficient bandwidth enhancement techniques are used to achieve wider bandwidth response i.e., 3.4-3.8 GHz within sub-6GHz. This system is realized over low-cost FR-4 laminate having dimensions of 64mm × 131mm. The fractal shape slotted radiators and open-ended square ring isolating structures achieves at least 25dB isolations among antenna pairs while maintaining wideband response. The optimum isolation, low-cost design profile, matched scattering parameters without compromising compactness and acceptable specific absorption rate makes this system a suitable candidate for 5G smart phone communications.

**INDEX TERMS** 5G, MIMO (Multi-Input-Multi-Output), Ring slot, Sub 6GHz, open-ended square ring (OESR), SAR

## I. INTRODUCTION

The Ever increase demand of wireless communications devices have brought significant improvements in communication networks. To solve the issues relating bandwidth limitations, higher data rates are provided by incorporating multi-input-multi-output (MIMO) systems [1]. MIMO technology is a promising technology for use in future 5G mobile terminals. It is worth mentioning that 5G will be the main developmental technology that will lead to a step-change in the capability enhancement of the mobile networks [2]. To achieve higher transmission rate MIMO antenna system incorporating large number of antennas should be adopted [3]. MIMO antenna system requires lower mutual coupling between antenna elements to reduce the effect of adjacent elements on system performance. On the other hand, when number of antennas are placed with minimum distance, raises unsought mutual coupling between antennas. To achieve maximum isolation, antennas are placed far apart. However, this increases overall size of the system, so it has always been a challenging task to arrange large number of antennas in a modern and compact sized smartphone with good isolation. Several techniques are used to suppress un-desired mutual coupling between the antennas. A capacitive loaded loop (CLL) metamaterial [4], parallel coupled-line (PCR) resonators [5], meandering [6] and etching slots from the ground forming defected ground structures (DGS) has proven effective for isolation.

enhancement [7]. Considerable works for 5G smartphones applications have been reported in literature. A multi-antenna array for 5G smartphones applications in [3] covers 3.5 GHz - 3.7 GHz for 5G communications. In [8], an eight-element complex array with impedance bandwidth of 3.4 GHz - 3.8 GHz is reported for the 5G mobile terminals. trade-off between isolation and compactness. A dual polarized 8×8 MIMO slot antenna in [9] comprises micro strip feedlines, square ring slot back element and rounded slot decoupling structures. In [10], an eight-port antenna system for 5G smartphone application is reported. This antenna has frequency band of 3.4 GHz - 3.6GHz with acceptable isolation on a larger size of 150mm × 70mm. An array of eight loop antenna elements operating at 3.5 GHz is reported in [11]. It achieves minimum isolation of 20dB over a 150mm × 75mm x 5.3mm sized array with 6 dB impedance bandwidth. This reported design offers maximum isolation of 10dB which affect the wireless performance. A multi feed multiple-input multiple-output (MIMO) antenna system operating in 5G frequency band is proposed in [12] with maximum isolation of 15dB. A self-decoupled 4-port multiple-input multiple-output (MIMO) antenna pair working in the midband of the 5G spectrum (3.5 GHz) for handheld device application is presented in [13] with isolation of -16dB. Despite smaller size both antennas reported in [12-13] fails to achieve isolation better than 20dB.

The Wideband Low-Profile antenna is designed to match Ultrathin 5G Smartphones in [15]. [16] is the Design and analysis of wideband MIMO antenna arrays for 5G smartphone application. In [17] an inverted L-shaped MIMO antenna with decoupled elements for smartphone application is designed. In [18], single feed CPW feed dual-band antenna is reported for ISM, WLAN, and Wi-Fi applications. A frequency reconfigurable octagonal patch loaded with stubs and diode is reported in [19]. This single feed antenna offers compact size and multiple resonances. A triangular quarter wave monopole antenna in [20] achieves wide bandwidth and flexibility. This single feed antenna provides sufficient bandwidth to achieve resonances at WLAN, Wi-Fi and C-band applications. In [21], a triband sub 6 GHz electronically tunable antenna is reported. The antenna is single feed and flexible Yet, all these do not consider isolations and multiport configurations and high bandwidth MIMO applications.

This paper contributes;

- A novel compact  $16 \times 16$  MIMO slot antenna system.
- The proposed MIMO system supports one of the most promising frequency band 3.4 GHz - 3.8 GHz for sub 6 GHz MIMO 5G communications. The fractal shape slotted radiators are designed to resonate at 3.5 GHz.
- The OESR isolation mechanism achieves at least 20 dB of isolation without compromising on compactness and impedance matching.
- All the MIMO performance parameters, its response on human body is investigated and found to be in acceptable limits.

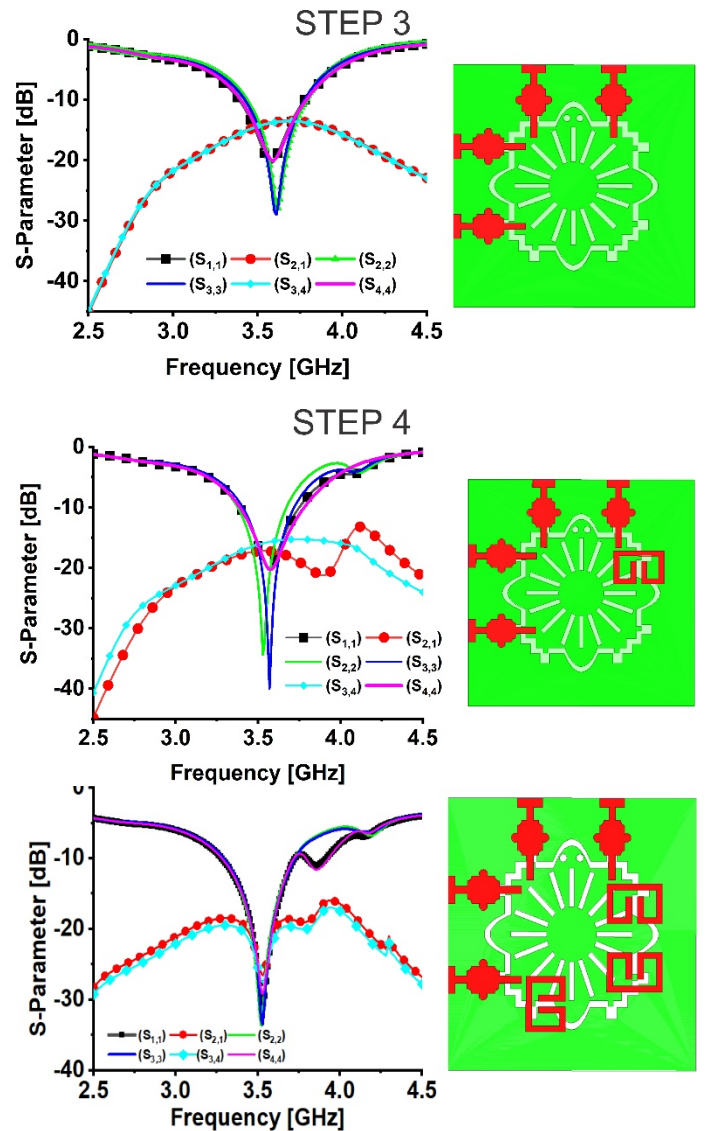
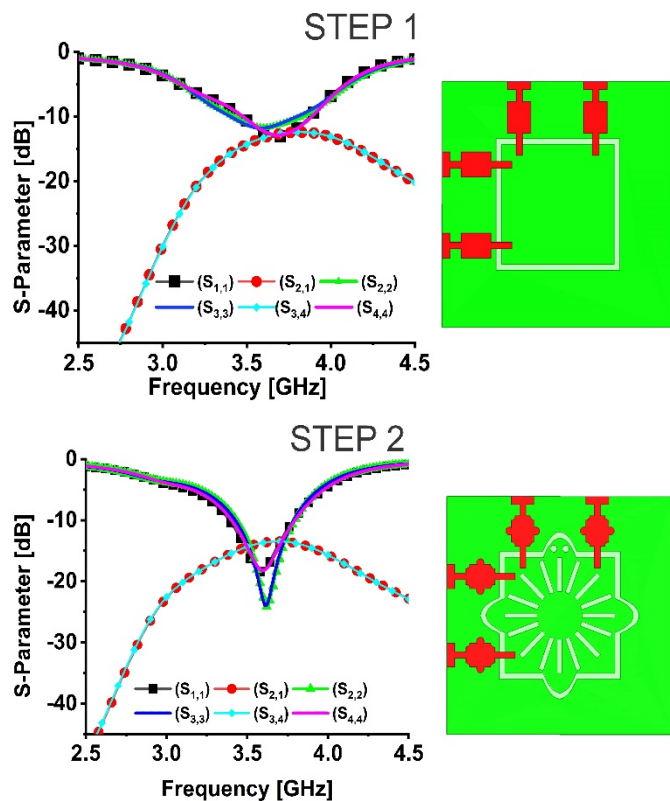


FIGURE 1. Design optimization of single element antenna

The rest of the paper is arranged as follows. In section II design configuration of single element antenna, Optimization, Parametrization along with its results are discussed. Section III covers the simulated and measured results of the proposed MIMO system. Section IV details the SAR analysis and finally section V concludes the papers.

## II. SINGLE ELEMENT ANTENNA

The proposed single element antenna is placed on a low cost and easily available 1.6 mm thick FR-4 laminate having compact dimension of 30mm x 30mm. The laminate has dielectric loss tangent 0.001 and relative permittivity of 4.4. The antenna configuration is composed of fractal shape slotted radiation element and four (two pairs) feeds placed orthogonally. Furthermore, three efficient open ended square ring (OESR) isolating structures are placed across the main radiation element. The step-by-step optimization of the proposed pairs are illustrated in Fig. 1.

**A. Antenna design**

A square ring slot are etched in the ground plane with tapered feed line on top of the substrate. These feeds are designed to obtain resonant response at 3.5GHz with no isolation as shown in the step 1. In step 2 beveling technique is applied on feed by adding circular arcs with elliptical slots are etched in ground plane to tune the resonant response. Furthermore, rectangular slots at 20° angles are etched from the ground to improve the impedance and isolation alongside. In addition to this, in step 3 a meandered profile is then introduced and etched from the ground to further improve of the impedance matching from 22dB to 30dB. OESR decoupling structure is then designed and placed across radiators in step 4. This improves the isolation but not on the desired frequency. Finally, in step 5 a couple of more decoupling OESRs are deployed across the radiators to achieves the isolation of at least 25dB at desired resonant frequency.

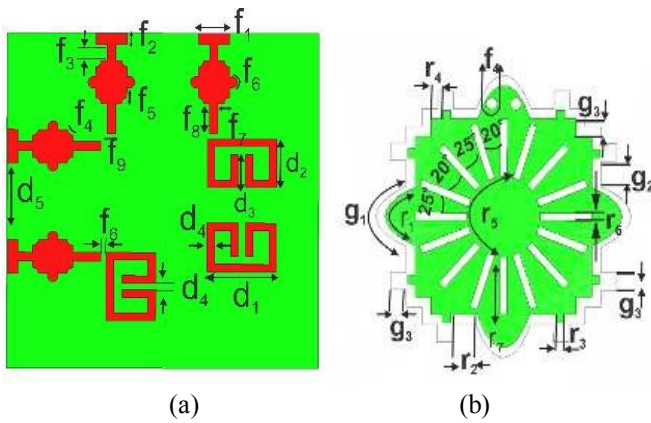


**FIGURE 2.** Single element design configuration (a) top-layer (b) bottom-layer

The complete design configurations of the proposed slot antenna are shown in Fig. 2. The optimization of scattering performance of antenna by varying the positions of OESR around the radiator is investigated as shown in Fig. 3. Results in Fig.4 for the different positions of OESR reveal that, antenna frequency response and the mutual coupling characteristics are highly depended on the position of the decoupling structure. Furthermore, as seen the fourth configuration Fig. 3(d) is the best position with matched impedance and isolation of at least -25dB on desired frequency as illustrated in Fig, 4(d).

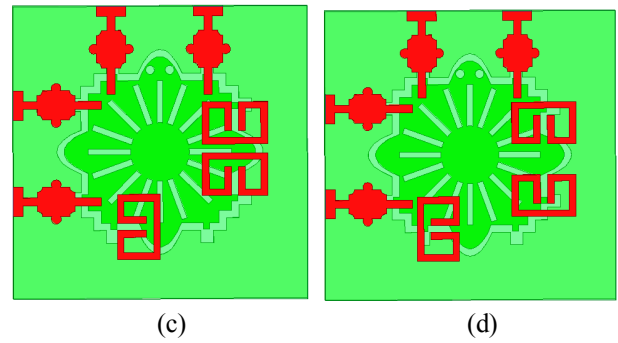
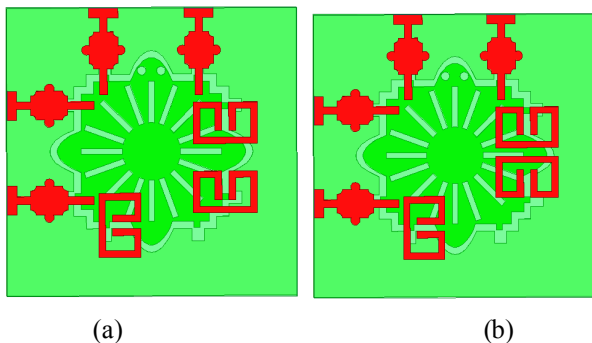


**FIGURE 3.** Positions of OESR across radiator

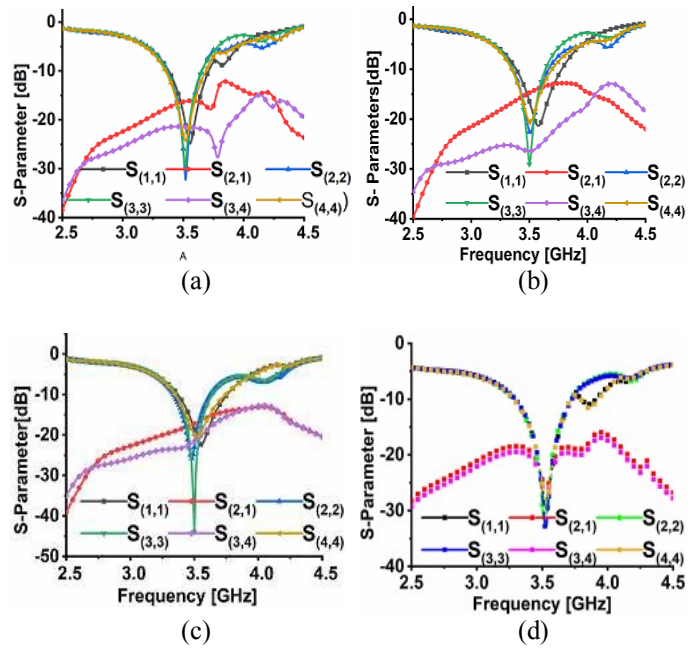


**FIGURE 4.** S-Parameter for different positions of OESR

**TABLE 1.** Design parameters

Var.	Value (mm)	Var.	Value (mm)	Var.	Value (mm)
f <sub>1</sub>	3	d <sub>1</sub>	6	r <sub>2</sub>	2.29
f <sub>2</sub>	1	d <sub>2</sub>	4.33	r <sub>3</sub>	0.645
f <sub>3</sub>	1.45	d <sub>3</sub>	2.95	r <sub>4</sub>	0.9675
f <sub>4</sub>	0.45	d <sub>4</sub>	0.715	r <sub>5</sub>	3
f <sub>5</sub>	0.941	d <sub>5</sub>	6.885	r <sub>6</sub>	0.6
f <sub>6</sub>	0.5	g <sub>1</sub>	3.5	r <sub>7</sub>	4.3
f <sub>7</sub>	0.602	g <sub>2</sub>	1.918	S	5.95
f <sub>8</sub>	2.7	g <sub>3</sub>	1.29	-	-
f <sub>9</sub>	0.8	r <sub>1</sub>	3.25	-	-

**B. Parametric optimizations**

The parametric optimization of OESR, feeding mechanism and slotted ground is presented in Fig. 5. The impact of

parameters  $d_3$  and  $d_4$  on isolation is analyzed in Fig.5(a) The variation of  $d_3$  and  $d_4$  shows that incremental increase shifts the optimum isolation to the center of the operation frequency. In Fig.5(b) a sharp resonant response is achieved by increasing  $f_6$  and  $f_8$  in a proportion i.e., values above the optimized, curve shifts towards lower frequencies with change in impedance from -35dB to -20dB. The parametric analysis of slotted ground in fig.5(c) reveals that, increase in the width of the slots  $r_6$  and  $g_1$  optimizes impedance matching over the desired frequency band.

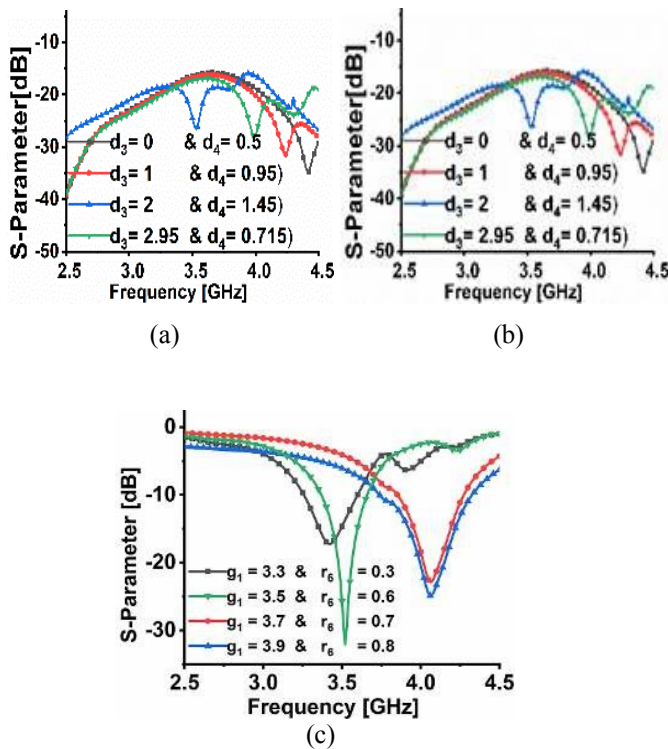


FIGURE 5. Design Parametrization (a) Decoupling structure (b) Feed (c) Slotted ground

**B. Current distribution of single element antenna**

The current distribution on proposed antenna pairs is evaluated across each active port at 3.5 GHz. As shown in Fig. 6. the current is saturated and absorbed by decoupling OSERs. Overall, a uniform J-surf distribution is achieved when ports and activated individually.

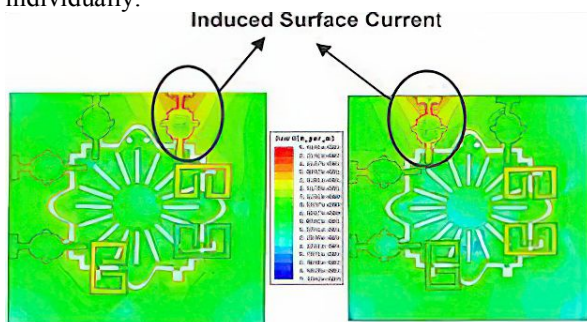


FIGURE 6. Surface current distribution at 3.5GHz.

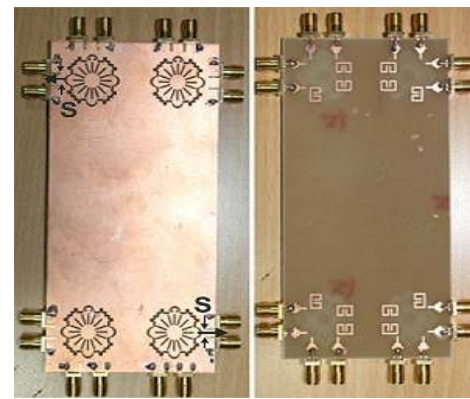
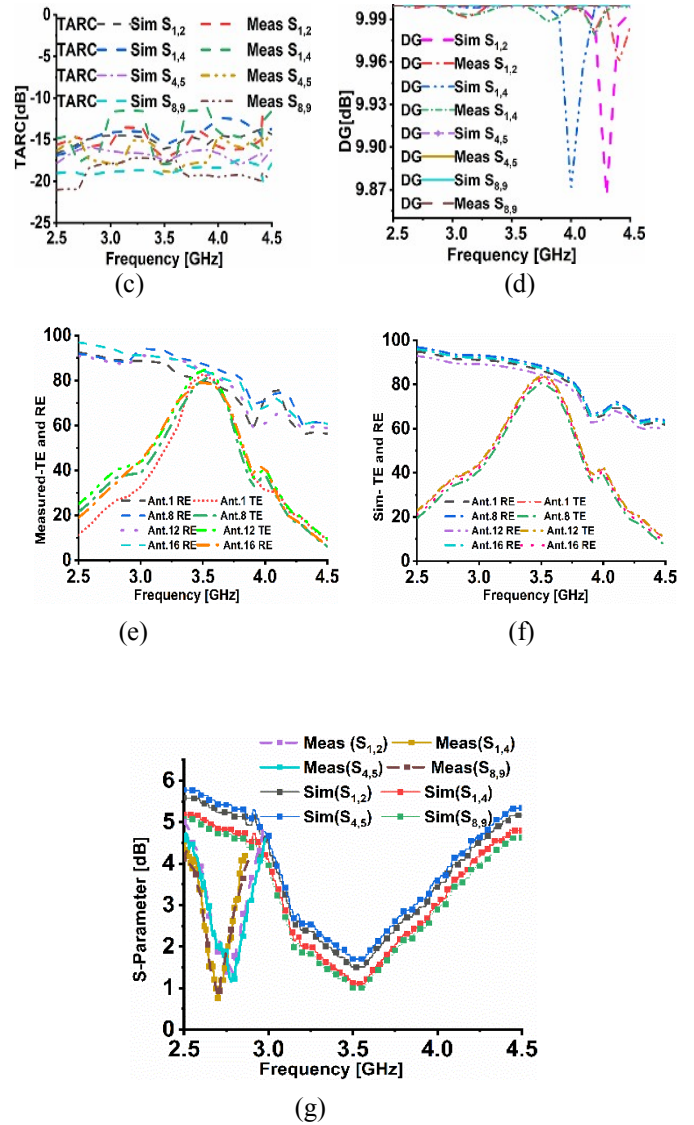
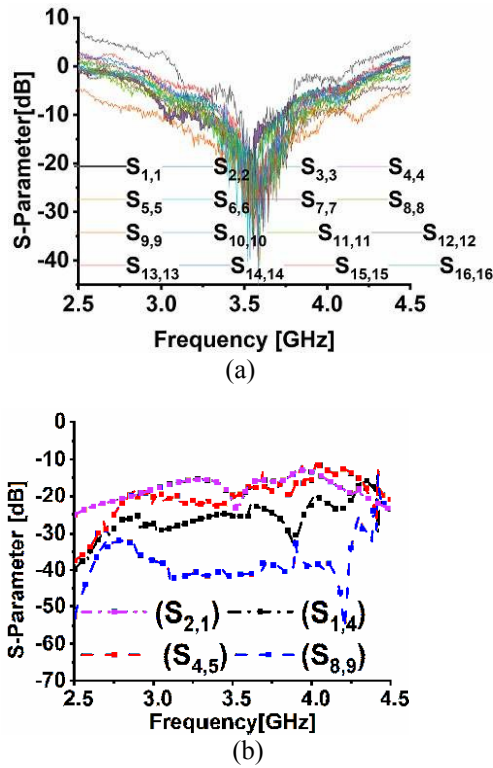


FIGURE 7. Fabrications and measurements (a) Bottom view and Top view (b) far field measurement.

**III. THE PROPOSED MIMO 5G SMARTPHONE ANTENNA**

To study the MIMO performance of the single element antenna, The proposed antenna pairs are extended to a 16- port MIMO antenna system having dimension of 64mm × 131 mm. Figure- 7 illustrates the top and bottom view of the fabricated MIMO antenna system along with its far field measurement setup.

The measured S-parameters including the return loss Fig8(a), and the mutual coupling characteristics of the proposed system is shown in Fig8(b), wideband impedance matching and at least 25dB isolation is also observed for the proposed 16 port array. As managing mutual coupling is critical, especially in applications where precise radiation patterns, high efficiency, and impedance matching are required. In this case decoupling structures and specialized antenna designs are used to reduce the impact of mutual coupling and get desired isolation shown as in Fig8(b).



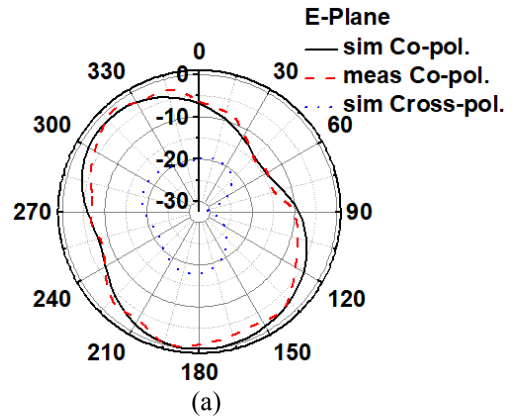
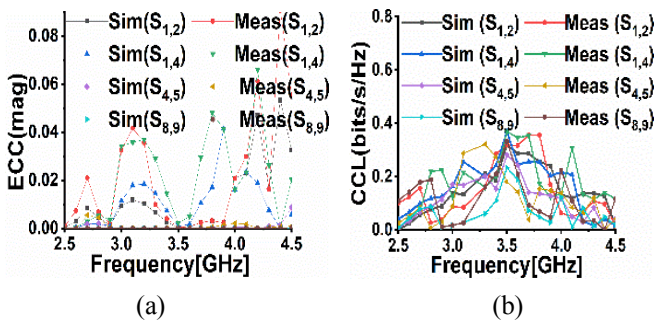
**FIGURE 8.** Measured S-parameters (a) Return loss (b) Isolation

**A. MIMO Performance**

MIMO performance of the proposed system is investigated by calculating Envelop Correlation Coefficient (ECC), Total active reflection coefficient (TARC), Diversity Gain (DG), mean effective gain (MEG), Total efficiencies (TE) and Radiation efficiencies (RE). Threshold value for ECC and CCL, less than 0.5, TARC < 0dB, DG < 9-10dB, and MEG < 3dB [14].

The proposed MIMO antenna achieved  $ECC < 0.1$ ,  $CCL < 0.2$ ,  $TARC < -15dB$ ,  $DG < 10dB$ , and  $MEG < 3dB$  as shown in Fig-9(a), (b), (c), (d) and (e). The simulated and measured results for radiation and total efficiencies are presented in figure 13(f) and 13(g). This system offers radiation efficiency of 85% and total efficiency more than 75% .

**FIGURE 9.** MIMO performance parameters (a) CCL (b) ECC (c) TARC (d) DG (e) measured TE and RE (f) sim-TE and RE (g) MEG



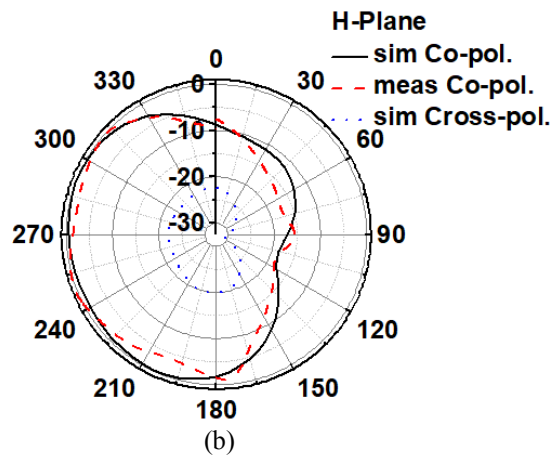
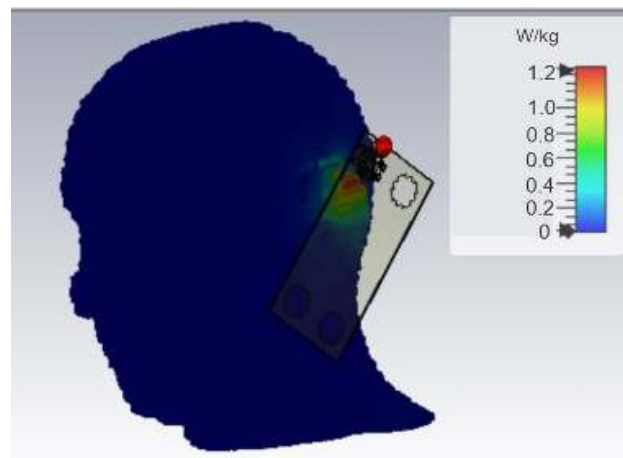
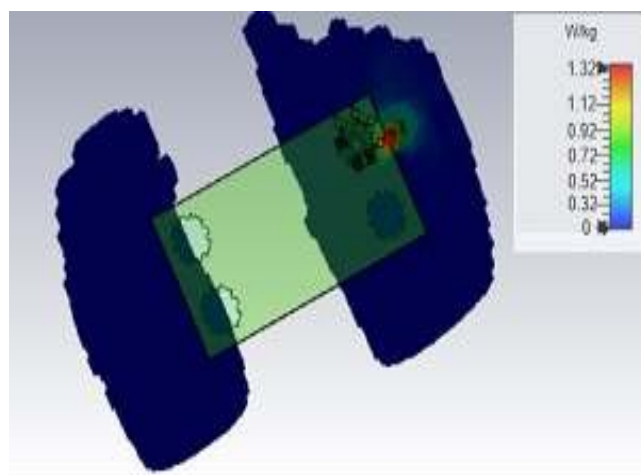


FIGURE 10. Radiation Patterns at 3.5 GHz (a) E plane (b) H-Plane



(b)

FIGURE 11. SAR evaluation at 3.5 GHz (a) hand (b) head.



(a)

TABLE 2. Comparison with existing literature.

Ref.	Size (mm)	Ports	Isolation (dB)	ECC (abs)	CCL (dB)	TARC (dB)	DG (dB)	MEG (dB)	TE (%)	RE (%)
[9]	150x75	8	-20	<0.01	-	-20	-	-	70	75
[10]	150x75	8	-17	>0.01 <0.02	-	-	-	-	-	65
[11]	150x75	8	-20	<0.4	-	-	-	-	-	33-47
[22]	150x75	8	-20	0.012	-	-	-	-	>60	70
[23]	140x70	8	-15	0.02	-	-	-	-	-	81
<b>Prop.</b>	<b>64x131</b>	<b>16</b>	<b>-30</b>	<b>0.01</b>	<b>0.1</b>	<b>-15</b>	<b>10</b>	<b>&lt;3</b>	<b>75</b>	<b>85</b>

### B. Radiation Characteristics

Fig. 10. shows the simulated and measured co and cross polarizations patterns of the proposed MIMO antenna system at 3.5 GHz. It may be inferred from the results that, cross polarizations at both planes are minimum and co-polarization of the system exhibits nearly omnidirectional radiation characteristics with pattern distortion to some extent owing to fabrication imperfections.

### C. User impact and SAR investigation

Specific absorption rate analysis is conducted for the proposed system on head, hands of the Voxel human body model. In figure 11, analysis conducted on operating frequency 3.5 GHz. The prescribed threshold from federal communication commission (FCC), SAR should be 1.6w/kg for 1 gram of tissue and according to the evaluated SARs of the proposed system into more than 1.32W/kg on 3.5GHz with reference power of 0.5W.

## IV. COMPARISON WITH EXSITINGWORK

Number of antennas are reported in literature for 5G smartphone applications. However, all of those either have compromises on compactness, isolation or fewer number of ports and MIMO performance parameters. The proposed 16-port MIMO antenna with reduced size has greater isolation with acceptable MIMO performance parameters. Detailed comparison with existing work is listed in Table 2.

## V. CONCLUSION

In this work, a compact and planar 16-port high resonant MIMO antenna system is presented. This system assures its suitability for 5G smart device applications owing to a compact arrangement. The designing approaches leads to antenna configuration by applying several techniques including but are not limited to beveling, chamfering, defected ground structures. Moreover, OESR isolation mechanisms are developed to isolate the proposed antennas. The isolation structure achieves overall isolation of not less than 25 dB. Notably, improved MIMO performance, acceptable SAR prove this system relevance for 5G communication devices.

## REFERENCES

- [1] MIMO antenna with defected ground structures for 5G cellular networks," *IET Microwaves, Antennas & Propagation*, vol. 12, no. 5, pp. 672-677, 2018.
- [2] H. Ullah, N. Gopalakrishnan Nair, A. Moore, C. Nugent, P. Muschamp, and M. Cuevas, "5G Communication: An Overview of Vehicle-to-Everything, Drones, and Healthcare Use-Cases," *IEEE Access*, vol. 7, pp. 37251-37268, 2019.
- [3] Y. Li, C.-Y.-D. Sim, Y. Luo, and G. Yang, "Multiband 10-antenna array for sub-6 GHz MIMO applications in 5-G smartphones," *IEEE Access*, vol. 6, pp. 28041-28253, 2018.
- [4] A. Jafarholi, A. Jafarholi and J. H. Choi, "Mutual Coupling Reduction in an Array of Patch Antennas Using CLL Metamaterial Superstrate for MIMO Applications," *IEEE Transactions on Antennas and Propagation*, vol. 67, no. 1, pp. 179-189, 2019.
- [5] K. S. Vishvakshnan, K. Mithra, R. Kalaiarasan and K. S. Raj, "Mutual Coupling Reduction in Microstrip Patch Antenna Arrays Using Parallel Coupled-Line Resonators," in *IEEE Antennas and Wireless Propagation Letters*, vol. 16, pp. 2146-2149, 2017.
- [6] S. Maddio, G. Pelosi, M. Righini, S. Selli, and I. Vecchi, "Mutual coupling reduction in multilayer patch antennas via meander line parasites," *Electron. Lett.*, vol. 54, no. 15, pp. 922-924, 2018.
- [7] K. Wei, J.-Y. Li, L. Wang, Z.-J. Xing, and R. Xu, "Mutual coupling reduction by novel fractal defected ground structure bandgap filter," *IEEE Trans. Antennas Propag.*, vol. 64, no. 10, pp. 4328-4335, 2016.
- [8] K.-L. Wong, C.-Y. Tsai, and J.-Y. Lu, "Two asymmetrically mirrored gap-coupled loop antennas as a compact building block for eight-antenna MIMO array in the future smartphone," *IEEE Trans. Antennas Propag.*, vol. 65, no. 4, pp. 1765-1778, 2017.
- [9] N. O. Parchin et al., "Eight-Element Dual-Polarized MIMO Slot Antenna System for 5G Smartphone Applications," *IEEE Access*, vol. 7, pp. 15612-15622, 2019.
- [10] G. Wei and Q. Feng *Progress in Electromagnetics Research C*, Vol. 99, 157-165, 2020.
- [11] Li, R.; Mo, Z.; Sun, H.; Sun, X.; Du, G. A Low-Profile and High isolate MIMO Antenna for 5G Mobile Terminal. *Micromachines*, vol. 11, no. 360. 2020.
- [12] Z. Ji et al., "Low Mutual Coupling Design for 5G MIMO Antennas Using Multi-Feed Technology and Its Application on Metal-Rimmed Mobile Phones," *IEEE Access*, vol. 9, pp. 151023-151036, 2021.
- [13] Abi T. Zerith Moses, Nesasudha Moses, Compact self- decoupled MIMO antenna pairs covering 3.4-3.6 GHz band for 5G handheld device applications, *AEU International Journal of Electronics and Communications*, vol. 141, 2021.
- [14] S. Shakir et al., "A Compact 8-Element 3D UWB Diversity Antenna System for Off Device Installation," *IEEE Access*, vol. 9, pp. 44117-44127, 2021.
- [15] H. Zhou, D. Wu, M. M. Zhu, Y. Qiu, G.L. Yu, H.M. Zhou, Wideband Low-Profile  $8 \times 8$  MIMO Antenna Based IFA Pair for Ultrathin 5G Smartphones. *Int. J. Antennas Propag.* pp. 5281470, 2022.
- [16] N. Sghaier, L. Latrach, Design and analysis of wideband MIMO antenna arrays for 5G smartphone application. *International Journal of Microwave and Wireless Technologies*, vol. 14 no. 4, pp. 511-523. 2022.
- [17] Hou J, Peng Y, Huang J, Wang Z, Denidni TA. MIMO 5G Smartphone Antenna with Tri-Band and Decoupled Elements. *Sensors*. 2023.
- [18] S. M. R. Jarchavi, M. Hussain, S. H. H. Gardezi, M. Alibakhshikenari, F. Falcone and E. Limiti, A Compact and Simple Prototype CPW-Fed Dual Band Antenna for ISM, Wi-Fi, and WLAN Applications," 2022 United States National Committee of URSI National Radio Science Meeting (USNC-URSI NRS), Boulder, CO, USA, pp. 30-31, 2022.
- [19] Hussain, M., Rizvi, S.N.R., Awan, W.A., Husain, N., Halima, Hameed, A. (2022). On-Demand Frequency Reconfigurable Flexible Antenna for 5Gsub-6-GHz and ISM Band Applications. In: Bennani, S., Lakhri, Y., Khaissidi, G., Mansouri, A., Khamlichi, Y. (eds) WITS 2020. Lecture Notes in Electrical Engineering, vol 745. Springer, Singapore.
- [20] W. A. Awan, M. Husain, M. Alibakhshikenari and E. Limiti, "Band Enhancement of a Compact Flexible Antenna for WLAN, Wi-Fi and C-Band Applications," 2021 International Symposium on Antennas and Propagation (ISAP), Taipei, Taiwan, 2021, pp. 1-2.
- [21] M. Hussain, EM Ali, WA Awan, N. Hussain, M. Alibakhshikenari, BS Virdee, Electronically reconfigurable and conformal triband antenna for wireless communications systems and portable devices. *PLoS ONE*. Vol. 17 no. 12, pp. e0276922, 2022.
- [22] A. Zhao and Z. Ren, "Size Reduction of Self-Isolated MIMO Antenna System for 5G Mobile Phone Applications," *IEEE Antennas and Wireless Propagation Letters*, vol. 18, no. 1, pp. 152-156, 2019.
- [23] Z. Yu, Y. Chen, Y. Xie and N. Guo. Eight-Element with h-Shaped Slot MIMO Antenna for 5G Applications. *Progress In Electromagnetics Research Letters*, vol. 90, pp. 7-13, 2020.